



Numerical Simulation and Experimental Validation of Microscale Fluid Flow Phenomena

Pankaj Negi,

asst. Professor, Department of Mechanical Engineering, Graphic Era Hill University,
Dehradun Uttarakhand India

Abstract.

Numerous industries, including microfluidics, biomedical engineering, and chemical processing, depend heavily on microscale fluid flow phenomena. Designing and improving microscale devices and processes requires a thorough understanding of and ability to predict these phenomena. The main objective of this study is to numerically simulate and experimentally verify microscale fluid flow processes. In this proposed approach method give a thorough analysis of microscale fluid flow in this work that combines numerical simulations and experimental methods. To simulate and forecast fluid behaviour at the microscale, we use computational fluid dynamics (CFD) models. The simulations take into account variables like viscosity, inertia, and intermolecular forces and are based on fundamental principles of fluid mechanics. Utilising cutting-edge microfluidic technology, experimental measurements are carried out to confirm the precision and dependability of the simulation results. In these studies, tiny fluid quantities are controlled, while flow patterns and velocities are tracked. The resulting experimental data are then contrasted with the outcomes of the numerical simulation in order to evaluate the simulation models' capacity for prediction. This paper show how the numerical simulation method may accurately forecast microscale fluid flow events. High levels of agreement between the simulation and experimental results validate the correctness and dependability of the computational models. This paper offers a thorough framework for numerical modelling and experimental validation, advancing the field of microscale fluid flow research. The study found that while the wetting performance had a substantial impact on the size distribution of liquid metal droplets, the droplet diameter showed less dependence on the contact angle. Monodisperse droplets developed as a result of a more hydrophilic behaviour. The numerical model and simulation outcomes show the possibility for precise droplet formation prediction in glass capillary microfluidic devices, especially for high surface tension liquids.

10440

Keywords: Interfacial tension, droplet generation, and a glass capillary microfluidic device

DOI Number: 10.48047/nq.2022.20.8.NQ221065

NeuroQuantology2022;20(8): 10440-10448

I. Introduction

Microscale fluid flow phenomena are important in many areas, such as chemical processing, biomedical engineering, and microfluidics. For

eISSN1303-5150

the design and improvement of microscale devices and processes, comprehension and precise prediction of these phenomena are essential. The main objective of this study is to



www.neuroquantology.com

numerically simulate and experimentally verify microscale fluid flow processes. This research intends to provide insights into the behaviour of fluids at the microscale by applying computational fluid dynamics (CFD) simulations based on fundamental principles of fluid mechanics, coupled with experimental measurements using cutting-edge microfluidic devices. Our comprehension of and modelling abilities in microscale fluid dynamics can be improved through the combination of numerical simulation and experimental validation. Liquid metals have exceptional low melting temperatures, low vapour pressures, excellent electrical and thermal conductivities, and high surface tension properties. These unique characteristics make them particularly intriguing for applications in functional composites, heat transfer management systems, and soft and flexible electronics. The use of liquid metals enables the fabrication of shape-memory alloys, interconnects, electrochemical sensors, and ultra-soft, compliant electrodes.

Symmetrical microdroplets, one of the many types of liquid metals, have drawn a lot of attention because of their potential for use in advanced functional electronics and microfluidic engineering gadgets. Highly monodisperse liquid metal microdroplet production has enormous application potential in periodic structures, optics, microfluidic actuators, self-powered acceleration sensors, radio frequency[1]. Therefore, it is crucial to have homogeneous size distribution in liquid metal droplets. Researchers can create groundbreaking innovations and improve performance in a variety of domains and applications by using the characteristics of liquid metals. These areas include microfluidics, electronics, and optics. Ultrasonication probes have been used to fragment bulk liquid metal into micro- to nanoscale spheres in the presence of ligands in a nonsolvent in order to increase manufacturing speeds[2]. The sonication procedure usually results in a wide size distribution ranging from a few hundred nanometers to several eISSN1303-5150

micrometres, even though it offers less control over droplet monodispersity than moulding approaches. Additionally, it is challenging to integrate the huge sonication devices with the detection and sensing technology used in lab-on-a-chip applications. An alternative method for creating liquid metal microspheres with customizable diameters involves using acoustic wave-induced forces to alter the interfacial tension of the metal with external excitation voltages in an acoustic field. The system might become more expensive and complex if signal generators and piezoelectric transducers are included. Decide on your preferred way of producing homogenous liquid metal microspheres on demand [3].

II. **Related work**

Recent studies have concentrated on numerical simulation and experimental validation of microscale fluid flow phenomena. The development of computational models and experimental methods to comprehend and characterise fluid behaviour at the microscale has advanced significantly. The development of this field has benefited from a number of important works[5].

Zhang et al. [7] published "Numerical simulation of microfluidic flows using the lattice Boltzmann method": The lattice Boltzmann method was used in this study to simulate microfluidic flows and analyse the effects of various factors on flow behaviour. The accuracy of the computational model was proven by validating the simulation results against experimental data.

Chen et al. [8] "Experimental characterization of microscale droplet formation in microfluidic devices": In order to research droplet formation in microfluidic devices, the scientists carried out experiments and examined the effects of numerous variables, including flow rates and channel geometries, on droplet size and formation. The consistency between the two methods was confirmed by comparing the experimental results with numerical simulations.

10441



Li et al.'s [9] titled "Numerical modelling and experimental validation of microscale heat transfer in microchannels": The study's main objectives were to numerically predict and experimentally verify heat transfer in microchannels. In order to assess temperature distributions, the researchers performed tests and created a computational model based on the finite element approach. The accuracy of the numerical model was shown by the simulation results, which were in good agreement with the experimental data.

Wang et al.[10] published a study titled "Validation of numerical simulation for electrokinetic flow in microchannels": The authors studied electrokinetic flow in microchannels and used experimental data to support numerical calculations. The study investigated how various electrokinetic phenomena affected fluid flow and used experimental validation to show the accuracy of the computational model.

Utilising a variety of techniques, numerical simulation and experimental validation of microscale fluid flow phenomena have been studied. Each technique has its own benefits and insights into the intricate behaviour of fluids at the microscale. The governing equations of fluid dynamics are solved using computational algorithms in the commonly used numerical simulation method known as fluid dynamics (FD) [11]. It allows for the prediction and visualisation of fluid behaviour in microscale systems, including velocity profiles, pressure distributions, and flow patterns. To effectively describe fluid flow, CFD simulations take into account variables including viscosity, inertia, and intermolecular forces [13].

The experimental method known as micro-PIV is used to evaluate fluid velocities at the microscale. It [14] entails introducing tracer particles into the fluid, lighting them with lasers, and observing their motion with high-speed cameras. Particle displacement over time can be used to calculate velocity fields and flow parameters, which is useful experimental information for verifying numerical simulations.

eISSN1303-5150

Techniques for flow visualisation offer in-depth understanding of fluid flow phenomena. Researchers are able to monitor and characterise flow patterns, vortex formation, and mixing processes in microscale systems using techniques like dye injection, laser-induced fluorescence, or micro-particle visualisation [17]. By offering a visual validation of the projected flow behaviour, flow visualisation experiments can be a useful addition to numerical models.

The majority of recent modelling studies have focused on the formation of droplets in water-in-oil or oil-in-water systems, whilst experimental studies have predominated the study of liquid metal microdroplets. However, numerical research has surprisingly little to say about the use of microfluidic technology to produce liquid metal microspheres, especially when a microfibre is introduced into the inner capillary to encourage stable droplet formation. This area of research is crucial for predicting droplet size and lowering production costs [7].

III. Proposed Methodology

A) Material:

In this experiment, an aqueous glycerol solution and a dispersed phase of liquid Galinstan metal were used in a continuous phase. In Shanghai, China, Aladdin provided the glycerol, and Sigma in St. Louis, Michigan, provided the Galinstan liquid metal. To prevent the spontaneous coalescence of the liquid metal droplets, a surfactant solution of Poly(vinyl alcohol) (PVA) was added to the glycerol solution. The PVA utilised was 87-89% hydrolyzed and had an average molecular weight (MW) ranging from 12,000 to 24,500 MW. Glycerol was added in a weight ratio of 10:2.9 to the 5% PVA aqueous solution. As a result, at room temperature, the dynamic viscosities of the continuous and dispersed phases were determined to be 0.044 Pas and 0.002 Pas, respectively [31]. The interfacial tension between the liquid metal and the aqueous glycerol solution was measured to be 0.4534 N/m [28]. The flow was steered using a stainless steel micro-needle with a 70 μ m diameter that was made by Zongsheng in

www.neuroquantology.com

10442



Harbin, China. Due to its outstanding resistance to chemical attack, rigidity, and high tensile strength, the stainless steel micro-needle was perfect for the experimental setup.

B) Experimental Environment Setup

The two tapered glass capillaries that made up the capillary-based co-flowing microfluidic device employed in this study were put together inside a square channel. Our earlier publication [31], which was published, has specific information about the device's manufacture and measurements. The square channel capillaries (810-9917) were provided by AIT Glass, Inc. of Largo, Florida, USA. With an axial distance of 100 m, the two inner capillaries were concentrically aligned. In addition, a

metallic needle known as a "micro-needle" was introduced along the orifice axis into the inlet capillary.

Please see Figure 1 for a visual representation of the experimental setup. The design of the microneedle-induced glass related capillary related device enabled controlled flow of the continuous and dispersed phases, a process that helped create liquid metal microdroplets. The glycerol and liquid metal were supplied by two microsyringe pumps (Harvard Apparatus, Holliston, MA, USA) equipped with gastight precision glass syringes (Hamilton, Bonaduz, Switzerland). The syringe pumps carefully controlled the flow rates of the two fluids.

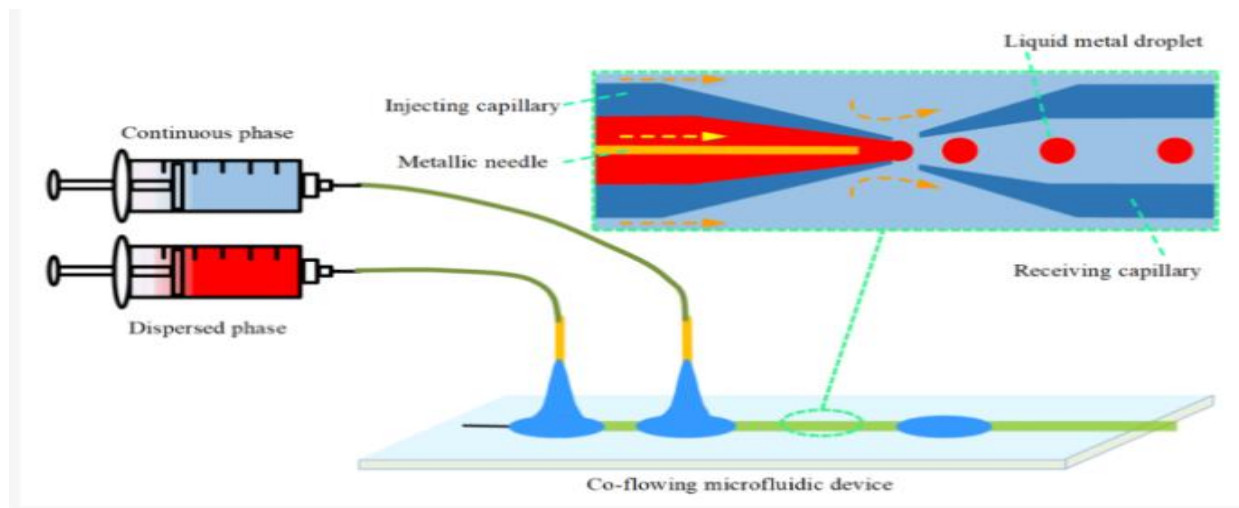


Figure 1: Diagram of the experimental setup for co-flowing microfluidics caused by microneedles.

The flow patterns and droplet formation in the microdevice were seen and recorded using an optical microscope and a high-speed charge-coupled device video camera. The microscope-camera setup allowed for real-time visualisation and recording of the fluid behaviour and droplet production processes inside the microdevice. In the total experimental setup, which included used microsyringe pumps for precise fluid, flow patterns and droplet formation were recorded and analysed using an optical microscope with a high-speed CCD camera.

IV. Numerical Simulation

1. Numerical Simulation

$$\rho(\partial u / \partial t) + \rho(u \cdot \nabla u) = \nabla \cdot [-pI + \mu \nabla(\nabla u + \nabla u^T)] + F$$

The creation of liquid droplet emulsions was simulated using a two-dimensional axisymmetric numerical model. The co-flowing capillary's transient fluxes of the continuous and scattered phases were taken into account by the model. The incompressible Navier-Stokes equation, which explains momentum conservation, and the continuity equation, which ensures mass conservation, regulate the fluid dynamics of the system. By resolving these equations, the model was able to investigate the droplet formation processes and represent the time-dependent behaviour of the fluid flows.



$$F_{\text{interfacial}} = \nabla \sigma$$

In this case, the gradient operator is, the interfacial tension between the two immiscible fluids is, and $F_{\text{interfacial}}$ stands in for the interfacial tension force.

Surface tension at the contact causes the interfacial tension force, which tends to reduce the surface area. The shape, stability, and behaviour of fluid droplets in the co-flowing tube are all significantly influenced by it. The said method effects provide the interfacial tension on droplet formation and behaviour can be precisely captured and reproduced by include the interfacial tension force in the numerical model.

$$F = \sigma \kappa \delta n$$

Where, κ and δ stand for the interface's curvature and the function focused across the interface between two nearby immiscible fluids, respectively, where σ is the surface tension coefficient. The flowing equation can be used to produce, and n is the unit interface normal vector pointing into the droplet.

$$\psi = -\nabla \cdot \epsilon \nabla \phi + (\phi^2 - 1)\phi$$

The parameter γ is used to control the thickness of the interface. By adjusting γ , the sharpness or smoothness of the interface can be controlled, allowing for a more accurate representation of the liquid-liquid interface profile.

$$\begin{aligned} \rho &= \rho_{\text{continuous}} + (\rho_{\text{dispersed}} - \rho_{\text{continuous}})\phi \\ \mu &= \mu_{\text{continuous}} + (\mu_{\text{dispersed}} - \mu_{\text{continuous}})\phi \end{aligned}$$

To properly trace the profile of the liquid-liquid interface and to smooth the fluid characteristics over the surrounding immiscible fluids, the phase field function is used. It ensures a continuous transition of fluid properties without sharp discontinuities, allowing for a more stable and reliable simulation.

Equations (7) and (8) can be used to calculate the density and dynamic viscosity in Equation (1). The density and dynamic viscosity are connected to the phase field function by these equations.

The fractional volume of the continuous and dispersed phases within each computational cell is represented by the phase field function (ϕ). In particular, when $\phi = 1$, it means that the dispersed phase has completely filled the cell. The fractional volume of the continuous and dispersed phases within each computational cell is represented by the phase field function (ϕ). In particular, when $\phi = 1$, it means that the dispersed phase has completely filled the cell. Conversely, when $\phi = 0$, it signifies that the cell is entirely occupied by the continuous phase. Intermediate values of $0 < \phi < 1$ represent the presence of a fluid-fluid interface within the cell. The values of the associated density and dynamic viscosity can be calculated by evaluating the phase field function at each computational cell. By taking into account the distribution of continuous and scattered phases, the presence of fluid-fluid interfaces within the system, and other factors, this enables precise estimation of the fluid characteristics in the numerical simulation.

2. Numerical Method

We used a commercial software programme (COMSOL Inc., Stockholm, Sweden) to conduct a numerical simulation in order to analyse the flow patterns and the creation of liquid metal microspheres. An axisymmetric model of the flow domain for the three-dimensional co-flowing capillary was used to create the simulation geometry. Figure 2 was used as a model for this geometry. In the simulation setup, the annular clearance between the inner circular capillary and the outer square capillary was filled with glycerol aqueous solution. On the other hand, the inner circular capillary received an injection of the bulk liquid metal from Galinstan. We wanted to comprehend the fluid behaviour and forecast the generation of liquid metal microspheres by modelling the flow dynamics and interfacial interactions within this geometry.



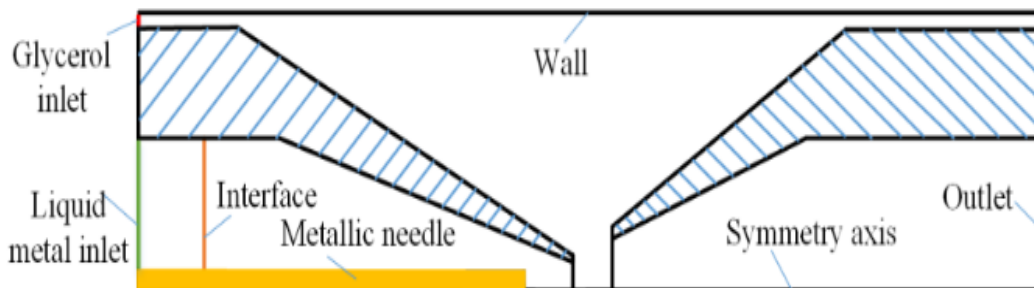


Figure 2: Simulation of the creation microspheres for liquid metal using a micro-needle-induced approach in a microchannel.

To explain droplet production, the simulation took into account the contact angle between the wetted wall and the droplets. The static contact angle between the two objects was measured in order to ascertain the wetting characteristics of Galinstan liquid metal on the microneedle. In Figure 3, this contact angle is shown. We also considered the contact angle (2)

between the liquid metal and the capillary wall in order to account for the interaction of the liquid metal with the environment. The initial contact angle values for the continuous phase's contact with the microneedle were set at $\pi/4$, and their initial values for their contact with the glass wall were set at $\pi/5$.

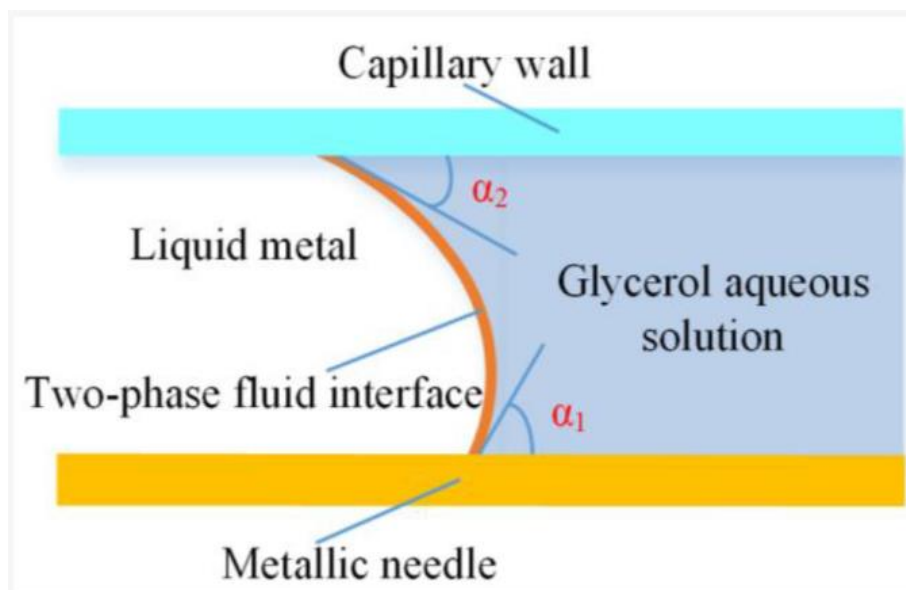


Figure 3: Contact angle between the liquid metal and metallic needle

The co-flowing capillary microchannel was simulated using a laminar flow model because of the low Reynolds number. In order to keep track of the interface structure of the two-phase immiscible fluids, a new variable called the phase field function was added. The momentum and phase field functions were calculated using the advection term. The mobility tuning parameter was set to 1 to

precisely control interface movement. The normal inflow speed, which was determined from the volume flow rate, served as the basis for the definition of the inlet conditions for the continuous phase and dispersed phase. With atmospheric pressure, the outflow boundary was configured as an open boundary. On the surface of the metallic needle and the sidewalls

of the capillary microchannel, non-slip conditions were imposed.

V. Result and Discussion

We conducted droplet formation simulations at various continuous phase flow rates while maintaining the dispersed phase flow rate constant at 12 L/min in order to verify the accuracy of our proposed phase-field method-based numerical model for two-phase flow. The continuous phase's flow rates varied from 0.060

to 0.120 mL/min. We compared the droplet sizes predicted by simulation with the results of the trials. According to the findings shown in Figure 4, the droplet size reduced as the continuous phase's flow rate rose. This pattern matched the experimental results Hutter [19] reported. Specifically, when the flow rates of the continuous phase and the scattered phase were 100 L/min and 10 L/min, respectively.

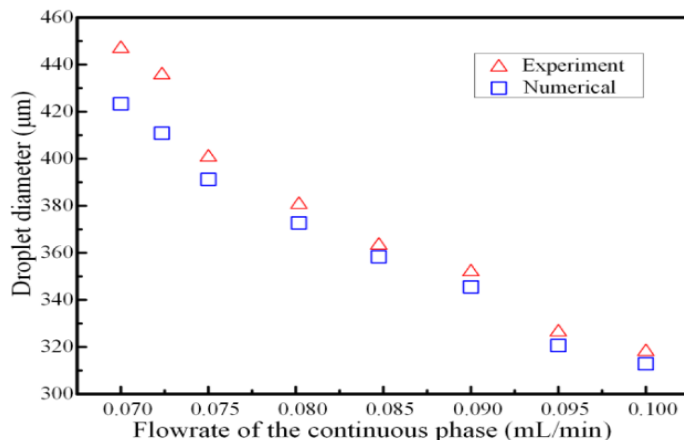


Figure 4: Comparison of numerical models and experimental data for the droplet diameter

Although the experiment's droplet sizes were slightly greater than the simulation's predictions, this disparity shrank as the glycerol aqueous solution's flow rate rose. This change may have been caused by variations in the velocity of the bulk liquid metal stream that was injected during the experiment. The generated liquid metal microspheres showed a high degree of monodispersity, as shown by simulation and experimental results, demonstrating the accuracy of our numerical model in predicting droplet sizes and the highly uniform nature of the generated liquid metal microspheres.

Particularly at the microscale, the interfacial tension between two immiscible fluids was essential to the emulsification process. To reduce the interfacial energy when the two fluids were in close proximity, they tended to form spherical droplets [14]. The interfacial tension of the nearby fluids had a significant impact on the breakdown mechanism and stability of droplets in the co-flowing capillary microfluidic system. The interfacial tension was crucial in keeping the liquid metal microspheres fixed to the capillary tip and preventing separation from the entering dispersed phase stream because liquid metal has a high surface tension.



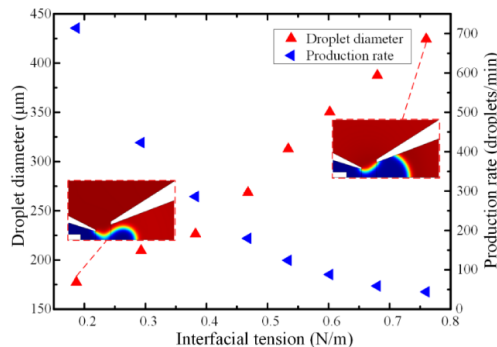


Figure 5: Influence of interfacial tension on droplet diameter and generation frequency when continuous and dispersed phase flow rates are compared

Figure 5 illustrates the relationship between interfacial tension and microdroplet formation, considering a fixed flow rate of 100 $\mu\text{L}/\text{min}$ for the continuous phase and 10 $\mu\text{L}/\text{min}$ for the dispersed phase. Compared to traditional oil droplet formation, the simulation results showed that the liquid metal droplet diameter was significantly larger, and the production rate was lower as the interfacial tension increased under the same conditions.

VI. Conclusion

In this study, we investigated microscale fluid flow processes, concentrating on liquid droplet formation, through numerical simulations and experimental validations. For the simulations, we created a two-dimensional axisymmetric numerical model and used a paid software programme. The simulations were carried out in a co-flowing capillary microfluidic device with the flow of Galinstan liquid metal as the dispersed phase and glycerol aqueous solution as the continuous phase. We were able to investigate the flow patterns and the creation of liquid metal microspheres through our numerical simulations. Systematically investigated were the effects of numerous parameters, including interfacial tension, wetting characteristics, viscosities, and flow rates. We further validated the accuracy and efficacy of our numerical model by comparing the simulation results with experimental data. The outcomes showed that the suggested numerical model accurately described how droplets develop in the co-flowing capillary device. In line with the results of the

experiments, we saw that the droplet size shrank as the continuous phase's flow rate increased. Interfacial tension's effect on droplet formation was also studied, and it was discovered that increased interfacial tension resulted in larger droplet sizes and slower production rates. This research advances our knowledge of microscale fluid flow dynamics and offers important tips for designing and perfecting microfluidic droplet production systems. This work's numerical simulations and experimental validations advance our understanding of liquid droplet dynamics and have applications in microfluidics, biomedical engineering, and materials research, among other areas.

References:

1. Dickey, M.D. Stretchable and Soft Electronics using Liquid Metals. *Adv. Mater.* 2017, 29, 1606425.
2. Deng, Y.; Liu, J. A liquid metal cooling system for the thermal management of high power LEDs. *Int. Commun. Heat Mass Transf.* 2010, 37, 788–791. [Google Scholar]
3. Chen, Y.; Zhou, T.; Li, Y.; Zhu, L.; Handschuh-Wang, S.; Zhu, D.; Zhou, X.; Liu, Z.; Gan, T.; Zhou, X. Robust Fabrication of Nonstick, Noncorrosive, Conductive Graphene-Coated Liquid Metal Droplets for Droplet-Based, Floating Electrodes. *Adv. Funct. Mater.* 2018, 28, 1706277.



4. Shay, T.; Velev, O.D.; Dickey, M.D. Soft electrodes combining hydrogel and liquid metal. *Soft Matter*. 2018, 14, 3296–3303.
5. Suarez, F.; Parekh, D.P.; Ladd, C.; Vashaee, D.; Dickey, M.D.; Öztürk, M.C. Flexible thermoelectric generator using bulk legs and liquid metal interconnects for wearable electronics. *Appl. Energy* 2017, 202, 736–745.
6. Sheng, L.; Teo, S.; Liu, J. Liquid-Metal-Painted Stretchable Capacitor Sensors for Wearable Healthcare Electronics. *J. Med. Biol. Eng.* 2016, 36, 265–272
7. Wang, X.; Zhang, Y.; Guo, R.; Wang, H.; Yuan, B.; Liu, J. Conformable liquid metal printed epidermal electronics for smart physiological monitoring and simulation treatment. *J. Micromech. Microeng.* 2018, 28, 034003.
8. Yu, Y.-Z.; Lu, J.-R.; Liu, J. 3D printing for functional electronics by injection and package of liquid metals into channels of mechanical structures. *Mater. Des.* 2017, 122, 80–89.
9. Mailen, R.W.; Dickey, M.D.; Genzer, J.; Zikry, M. Effects of thermo-mechanical behavior and hinge geometry on folding response of shape memory polymer sheets. *J. Appl. Phys.* 2017, 122, 195103.
10. Wissman, J.; Dickey, M.D.; Majidi, C. Field-Controlled Electrical Switch with Liquid Metal. *Adv. Sci.* 2017, 4, 1700169.
11. Baek, S.; Park, U.; Choi, I.H.; Kim, J. Pneumatic RF MEMS switch using a liquid metal droplet. *J. Micromech. Microeng.* 2013, 23, 055006.
12. McLanahan, A.R.; Richards, C.D.; Richards, R.F. A dielectric liquid contact thermal switch with electrowetting actuation. *J. Micromech. Microeng.* 2011, 21, 104009.
13. Tang, S.-Y.; Khoshmanesh, K.; Sivan, V.; Petersen, P.; O’Mullane, A.P.; Abbott, D.; Mitchell, A.; Kalantar-zadeh, K. Liquid metal enabled pump. *Proc. Natl. Acad. Sci. USA* 2014, 111, 3304–3309.
14. Tang, S.-Y.; Sivan, V.; Petersen, P.; Zhang, W.; Morrison, P.D.; Kalantar-zadeh, K.; Mitchell, A.; Khoshmanesh, K. Liquid Metal Actuator for Inducing Chaotic Advection. *Adv. Funct. Mater.* 2014, 24, 5851–5858.
15. Zhang, B.; Zhang, L.; Deng, W.; Jin, L.; Chun, F.; Pan, H.; Gu, B.; Zhang, H.; Lv, Z.; Yang, W.; et al. Self-Powered Acceleration Sensor Based on Liquid Metal Triboelectric Nanogenerator for Vibration Monitoring. *ACS Nano* 2017, 11, 7440–7446.
16. Zou, L.; Withayachumnankul, W.; Shah, C.M.; Mitchell, A.; Bhaskaran, M.; Sriram, S.; Fumeaux, C. Dielectric resonator nanoantennas at visible frequencies. *Opt. Express* 2013, 21, 1344–1352.
17. Hashimoto, M.; Mayers, B.; Garstecki, P.; Whitesides, G.M. Flowing Lattices of Bubbles as Tunable, Self-Assembled Diffraction Gratings. *Small* 2006, 2, 1292–1298.
18. Yu, J.; Yang, Y.; Liu, A.; Chin, L.; Zhang, X. Microfluidic droplet grating for reconfigurable optical diffraction. *Opt. Lett.* 2010, 35, 1890–1892.
19. Pollack, M.G.; Shenderov, A.D.; Fair, R.B. Electrowetting-based actuation of droplets for integrated microfluidics. *Lab Chip* 2002, 2, 96–101.
20. Mohammed, M.; Xenakis, A.; Dickey, M. Production of Liquid Metal Spheres by Molding. *Metals* 2014, 4, 465–476.
21. Tang, S.Y.; Ayan, B.; Nama, N.; Bian, Y.; Lata, J.P.; Guo, X.; Huang, T.J. On-Chip Production of Size-Controllable Liquid Metal Microdroplets Using Acoustic Waves. *Small* 2016, 12, 3861–3869.

